Analytical Methods

In Situ Hemolysis in a Three-Dimensional Paper-Based Device for Quantification of Intraerythrocytic Analytes

Journal:	*Analytical Methods*
Manuscript ID	AY-ART-10-2019-002292.R1
Article Type:	Paper
Date Submitted by the Author:	22-Nov-2019
Complete List of Authors:	Baillargeon, Keith; Tufts University, Chemistry Bricknell, Jordan; Tufts University, Chemistry Mace, Charles; Tufts University, Chemistry; Laboratory for Living Devices

In Situ Hemolysis in a Three-Dimensional Paper-Based Device for Quantification of Intraerythrocytic Analytes

Keith R. Baillargeon, Jordan R. Bricknell, and Charles R. Mace*

Department of Chemistry, Laboratory for Living Devices, Tufts University, Medford, MA 02155

* corresponding author email: charles.mace@tufts.edu

Abstract

Blood-based diagnostics require various forms of sample preparation depending on the analyte of interest, which can include plasma separation and cellular lysis. Specifically, assays that require the release of intraerythrocytic analytes (e.g., detection of malaria antigens, dehydrogenases, and hemoglobin) require the rupture of red blood cells prior to analysis. Associated handling steps and additional fluid manipulation complicates the user-experience by adding time, potential for contamination error, and reagent waste. In this work, we demonstrate an in situ chemical hemolysis treatment coupled with a paper-based device for the quantification of liberated hemoglobin without using a hemolytic buffer. In contrast to traditional hemolytic methods that use a buffered solution of saponin, a surfactant, we dried saponin within our device to lyse red blood cells without diluting the sample. The optimal treatment condition for hemolysis of blood samples with hematocrit values ranging from 20–50% was 10.6 μg saponin/cm^2. Establishing a relationship between saponin and zone area potentially allows this in situ hemolysis treatment to be translated to other paper-based devices with different geometries. For samples with hematocrit values below 40%, we achieved quantitative hemolysis. Samples with higher hematocrits (e.g., 40–50%) experienced a lesser extent of hemolysis (80–85%), which we attribute to the increased number of red blood cells present in samples with elevated hematocrits. The in situ chemical hemolysis treatment described here could potentially be integrated with a multiplexed paper-based microfluidic device to permit multiple sample preparation techniques on a single sample of blood without additional off-chip user steps.

1. Introduction

Point-of-care diagnostics promise a cost-effective, equipment-free, and operationally simple user experience. While advances in the development of diagnostic assays at the point-of-care have accelerated over the past decade [1–5], sample preparation has lacked similar innovation [6]. Operators are often required to perform off-chip dilutions [7–9], sequential reagent additions [10], and even separations to isolate blood components (e.g., plasma or serum). This approach of segmented sample preparation requires multiple sample collections and multiple individual tests to be performed. Unfortunately, this approach inhibits adoption of blood-based assays at the point-of-care by adding time, complexity, and reagent waste. For example, testing for intracellular contents of red blood cells (RBCs) requires cell membrane disruption prior to conducting an assay. This is commonly achieved using a hemolytic buffer in conjunction with lateral flow tests. However, application of a hemolytic buffer following sample addition results in complete hemolysis of the blood sample and eliminates the possibility of multiplexed analysis from a single sample of blood (e.g., whole blood, purified plasma, and hemolysate preparation from a single blood sample).

Successful integration of on-chip hemolysis into traditional microfluidic point-of-care devices has required mechanical [11, 12], thermal [13, 14], and chemical [15–17] mechanisms to disrupt RBC membranes. While these approaches are widely employed in laboratory settings, they are limited to the benchtop due to the need for external pumps for fluid manipulation [18,19]. In contrast, paper-based microfluidics offer the advantage of controlling fluid flow by capillary action. Patterning paper with hydrophobic barriers provides further utility by spatially separating reagents within a device to perform multi-step reactions [20–23]. Paper-based devices, as a platform, are highly adaptable to a variety of diagnostic assay formats [24] and address many of the challenges associated with point-of-care settings.

Sample preparation (i.e., hemolysis) was previously integrated into both immunochromatographic [25] and origami-style paper-based microfluidic [26] devices. In both

devices, Triton X-100 was dried and stored on-chip in a thick porous material. Effective hemolysis was achieved after rehydration of Triton X-100 with the addition of a liquid sample and a short incubation period. Surfactants such as Triton X-100, however, are incompatible with hydrophobic wax barriers, which limits this approach to unpatterned media similar to commercially available immunochromatographic strips. An alternative approach is utilized by the BinaxNOW malaria immunochromatographic strip by Abbott, which qualitatively detects malaria antigens released from red blood cells [27]. The BinaxNOW immunochromatographic test achieves on-chip hemolysis through the addition of a running buffer containing detergent for hemolysis following initiation of the assay, effectively destroying the integrity of the sample for alternative analysis (e.g., purified plasma or whole RBCs). Incorporating controlled hemolysis directly into a multi-layered, wax-patterned paper-based device would permit a new suite of diagnostic assays including intraerythrocytic analytes (e.g., detection of malaria antigens and dehydrogenases) in addition to plasma and whole cell analytes by spatially separating components for sample preparation.

Herein, we describe a surfactant-mediated hemolytic treatment integrated with a wax-patterned, paper-based microfluidic device and demonstrate in-line quantification of the intraerythrocytic analyte hemoglobin without the use of a hemolytic buffer. We utilize the surfactant, saponin, stored in paper to rupture RBC membranes [28, 29] while maintaining hydrophobic wax barriers to control fluid flow in three-dimensions. Inclusion of a plasma separation membrane removes RBC membrane fragments to prevent clogging of the device. We evaluate our in situ hemolysis approach by quantifying liberated hemoglobin with respect to saponin concentration and hematocrit. This treatment could also be stored within multiplexed paper-based microfluidic devices to allow multiple sample preparation techniques to be performed on a single sample of blood without additional off-chip user steps, generating excessive reagent waste, or adding lengthy incubation times.

2. Experimental Design

2.1 Device Design and Fabrication

Our three-dimensional, paper-based device comprises three layers: (i) sample addition and hemolysis, (ii) RBC membrane exclusion, and (iii) lateral channel (**Fig. 1B**). Addition of whole blood initiates the assay, rehydrating the hemolytic reagent—saponin—for in situ hemolysis. Disruption of the RBC membrane releases intraerythrocytic contents into the plasma and results in an excess of membrane fragments, which are retained by a plasma separation membrane to prevent clogging of the paper channel below. The plasma carrier fluid then facilitates the transport of soluble, intraerythrocytic contents through the lateral channel by capillary action. The RBC membrane exclusion layer (ii) is a polysulfone material with an asymmetric pore structure used to passively filter cells and produce purified plasma (Pall Corp. Vivid GR). The remaining layers of the device were fabricated from Whatman Grade 4 qualitative chromatography paper for its fast wicking rate.

We used Adobe Illustrator to design each paper layer of this device and printed the hydrophobic wax barriers using a Xerox ColorQube 8580 wax printer. We used a Promo Heat CS-15 T-shirt press (45 seconds at 280 ˚F) to form hydrophobic barriers through the full thickness of the patterned chromatography paper (Whatman grade 4), which defined the storage zones for dried assay reagents. We used double-sided permanent adhesive (Flexmount Select DF021621) to maintain contact between each layer of the device and Fellowes transparency laminate to protect the stored reagents from environmental contaminants and user interference.

2.2 Evaluation of Quantitative, In Situ Hemolysis

Blood was used within 48 hours after initial receipt to minimize effects of cell morphology changes, which could affect flow of blood samples in paper [30]. We defined extent of hemolysis as the ratio of liberated hemoglobin to total hemoglobin in a sample of blood using an elution method (**Fig. 1A**). First, we calibrated the paper-based device (**Fig. 1B**) with hemolysate

standards (**Fig. 1C**). Next, we prepared whole blood samples at various hematocrit values and concentrations of hemoglobin, applied them to the sample addition layer, and allowed the sample to saturate the end zone of the lateral channel. In accordance with the WHO recommendation, we used a standard office hole punch to remove a 6-mm diameter punch from the end of each lateral channel containing the liberated intraerythrocytic contents [31]. We then eluted each punch in 1.0 mL Drabkin's reagent for 30 minutes before quantifying the concentration of hemoglobin by UV-vis. The Drabkin's reagent converts all forms of hemoglobin to a single, stable form of hemoglobin (i.e., cyanmethemoglobin), which can be reproducibly measured at 540 nm [32]. While the Drabkin's assay is designed to lyse samples of whole blood, inclusion of the PSM ensures no intact cells can enter the paper channel. As a result, samples obtained by elution from the paper punch at the terminal zone of the channel contain no additional cells to lyse and any detected hemoglobin will only be the result of on-device hemolysis. We prepared hemolysate controls off-chip to represent complete hemolysis and provided the value for total hemoglobin. We used lyophilized hemoglobin standards rehydrated with diH_2O (18 MΩ) to construct calibration curves over a range of 3–18 g/dL. We determined the limit of detection (LOD) for the Drabkin's assay using isolated plasma obtained by centrifugation of whole blood (n=20).

2.3 Live Subject Statement

We obtained washed human red blood cells (type O+) suspended in Alsever's solution from Innovative Research (Novi, MI). Blood was drawn by the vendor from healthy donors in an FDA-licensed facility. We obtained samples of whole blood from Research Blood Components (Woburn, MA). The vendor follows American Association of Blood Banks guidelines for all donors, which includes IRB approved consent to the use of collected blood for research purposes. All research was approved by the Tufts University Institutional Biosafety Committee.

3. Results and Discussion

3.1 Determination of Optimal Lytic Agent

We aimed to integrate our chemical hemolysis approach with a paper-based device to eliminate the burden of sample preparation at the point-of-care. Fabricating paper-based devices with hydrophobic wax barriers is a simple and effective method which allows for rapid prototyping of inexpensive devices [33]. Reagents stored within these devices must be compatible with analytes of interest (e.g., do not denature proteins) as well as the hydrophobic wax barriers (i.e., do not penetrate the wax). We surveyed surfactants (e.g., Triton X-100, sodium dodecyl sulfate SDS, CHAPS, and saponin) at various concentrations for (i) efficacy of hemolysis and (ii) compatibility with hydrophobic wax barriers. While surfactants such as Triton X-100 and SDS are effective at lysing RBCs, they are harsh surfactants that can denature target analytes. Additionally, these surfactants are incompatible with wax barriers. In contrast, the integrity of wax barriers is maintained in the presence of both CHAPS and saponin. We compared the efficacy of hemolysis for both CHAPS and saponin in solution at various concentrations using the decrease in packed RBC volume at the bottom of a microhematocrit tube. At a hematocrit value of 45%, CHAPS yielded a maximum of 70.4% hemolysis with a concentration of 12.5 mg/mL (**Fig. S1A**). Increasing the concentration of CHAPS did not result in a greater extent of hemolysis. In contrast, at a hematocrit value of 45%, saponin had a much greater efficacy at 91.4% hemolysis using a concentration of 1.6 mg/mL saponin in solution (**Fig. S1B**). We decided to use saponin, rather than CHAPS, because saponin yielded a higher extent of hemolysis in solution.

3.2 Characterization of In Situ Hemolysis

Chemical hemolysis is initiated by application of a blood sample. No additional buffer is required for hemolysis or sample flow. To evaluate the extent of hemolysis in our paper-based device (**Fig. 1B**), we quantified the concentration of hemoglobin transported to the terminal zone of the lateral channel using our elution method (**Fig. 1A**). Once the hemolysate saturated the

terminal zone, we removed a 6-mm punch of paper containing the intraerythrocytic analytes and immediately submerged the punch in 1.0 mL of Drabkin's reagent on a rotisserie for 30 minutes. Since the Drabkin's assay for total quantitation of hemoglobin requires accurate dilution of the sample, we first compared the calibration data in our paper-based device with matched liquid samples using a reference method (**Fig. 1C**). Hemoglobin standards prepared over the physiological range (3–18 g/dL) were directly (i) applied to the paper-based device and (ii) diluted in 1.0 mL of Drabkin's reagent. The sample volumes were 20 μL and 4 μL, respectively. Both methods of quantitation were analyzed by linear regression and yielded R-squared values greater than 0.99. The LOD was calculated as 2.9 g/dL hemoglobin in purified plasma using the reference method calibration curve. While both calibration curves demonstrated excellent linearity over the physiological range of hemoglobin, the slopes differed between the two methods of quantitation (**Fig. 1C**). Our paper-based device was less sensitive than the reference method with slopes of 0.0101 and 0.0127, respectively. We attribute this decrease in sensitivity to a decreased sample volume eluted from the paper punch. To confirm the volume of sample obtained from the paper punch, we constructed calibration curves using the reference method and liquid samples of hemoglobin at 2, 3, 4, and 5 μL. These volumes correspond to dilution factors of 1:500, 1:333, 1:250, and 1:200, respectively. Using the slopes obtained from these calibration curves, we estimated that our paper punch contains a sample volume of 3.4 μL (**Fig. 2**). To account for the sample volume discrepancy between our paper punch and liquid reference samples, we calculated a correction factor by comparing the slopes of the reference calibration the elution calibration (**Fig. 1C**). Applying this correction factor of 1.26 to the concentration of hemoglobin obtained from preparing samples using our paper-based device allows for accurate quantitation of hemoglobin (i.e., comparable to the concentration of hemoglobin obtained from the reference method) in blood samples.

In order to evaluate the extent of hemolysis, hemolyzed samples must saturate the terminal zone of the lateral channel prior to elution. We prepared hemolysate controls off-chip

over a physiologically relevant range of hematocrits (i.e., 25%, 40%, and 55%) and added them to devices without saponin dried onto the sample addition layer. The hemolysate controls correspond to 7.8, 13.6, and 19.1 g/dL hemoglobin, respectively. Initially, samples of blood with high hematocrits (e.g., 55%) and high concentrations of hemoglobin (e.g., approximately 20 g/dL) did not saturate the terminal zone of the lateral channel following the release of intraerythrocytic contents from RBCs. To improve filling of the device at high hematocrits and high concentrations of hemoglobin, we first varied the input volume of the sample. Increasing the sample volume from 20 μL to 40 μL slightly increased device filling and sample flow at low and normal hematocrits, but samples with high hematocrits still did not saturate the terminal zone. We previously determined that treating paper-based devices with ethylenediaminetetraacetic acid (EDTA) improved the flow of blood with respect to the hematocrit [34]. Similarly, we treated the sample addition zone in our hemolysis device with 0.5 M EDTA to improve blood flow. Treating the sample addition layer with EDTA ensured all hemolysate controls were transported to the end of the lateral channel regardless of hematocrit with a sample volume of 40 μL (**Fig. 3**).

3.3 Efficacy of In Situ Hemolysis at Various Hematocrits

Extent of hemolysis is dependent on the number of surfactant molecules per RBC, which is directly related to the hematocrit value (i.e., ratio of packed RBC volume to total blood volume). To account for a higher number of RBCs in blood samples at high hematocrits, we varied the concentration of saponin dried onto the sample addition layer and measured the extent of hemolysis over a physiological range of hematocrit values (20–50%). Blood samples were prepared with different hematocrits by increasing or decreasing the volume of plasma. All samples were warmed to 37 ˚C prior to analysis. The initial concentration of total hemoglobin was measured using the reference method. Extent of hemolysis was expressed as the ratio of liberated hemoglobin eluted from the terminal zone to the total concentration of hemoglobin in the sample. Paper-based devices were treated with 2.5–7.0 μL of 50% w/v saponin and 0.5 M

EDTA, corresponding to 4.4–12.4 μg saponin/cm^2. For all blood samples, we observed a positive relationship between extent of hemolysis and concentration of saponin between 4.4–10.6 μg saponin/cm^2 (**Fig. 4A**). Further increasing the concentration of saponin above 10.6 μg saponin/cm^2 resulted in a lesser extent of hemolysis for all blood samples. Above this critical concentration of 10.6 μg saponin/cm^2, rehydration becomes a limiting factor, which results in fewer RBCs interacting with the saponin and a subsequent lesser extent of hemolysis.

As an alternative to paper, which is composed of an interconnected network of heterogeneous pores, we investigated drying saponin onto a uniform mesh with a single open pore size (20 μm). In this configuration, the mesh concentrates all dried mass of saponin onto the two faces (top and bottom) and within each pore of a thin sheet rather than distributing the saponin throughout the thickness of a porous material. As a result, we expect the effective concentration of saponin to be higher in devices comprising meshes in contrast to papers. We compared the effectiveness of both mesh and paper to promote hemolysis. In this set of experiments, 3 mg of saponin (6 μL of 500 mg/mL) was applied to a 6-mm wide zone (28.3 mm^2): (i) the Whatman 4 paper has a thickness of 205 μm and a porosity of 71.3% (as determined by X-ray microcomputed tomography) [35,36] and (ii) the mesh has a thickness of 60 μm and an open area of 13% [37]. As a result, the effective concentration of saponin upon rehydration is 12.5-fold higher in the mesh device than the paper device (9.1 mg/mm^3 vs. 0.7 mg/mm^3). However, mesh devices did not result in a higher extent of hemolysis. Instead, hemolysis decreased for blood samples at 35% and 55% Hct (**Table S1**), which suggests that rehydration, and not solely the amount of available lysis agent, plays a role in the efficacy of hemolysis in these devices.

Optimal hemolysis was achieved by treating the sample addition layer (Whatman grade 4) with 6 μL of 50% w/v saponin, which corresponds to 10.6 μg saponin/cm^2 (**Fig. 4B**). For samples with hematocrit values below 40%, we achieved quantitative hemolysis (i.e., 100% hemolysis). Samples with higher hematocrits (e.g., 40–50%), experienced a lesser extent of

hemolysis. We attribute this lesser extent of hemolysis to the increased number of RBCs present in samples of blood with elevated hematocrits. Considering the low variance observed for each sample (4–11% SEM), a correction factor could be applied to quantitative assay results if the hematocrit value is known to account for the lesser extent of hemolysis. For example, if a sample of blood with a known hematocrit of 50% is applied to our device and we quantify the concentration of hemoglobin in the hemolysate as 16.3 g/dL (eluted from the paper punch), we can apply a correction factor of 1.2 to increase the concentration of hemoglobin assuming that only 80% of the RBCs are lysed at this hematocrit. Applying this correction factor would effectively account for the 20% of RBCs that are not lysed and result in a calculated concentration of hemoglobin (ca. 19.6 g/dL), which is approximately 4% higher than the theoretical reference value (ca. 18.8 g/dL).

4. Conclusions

We aimed to integrate a surfactant-mediated hemolytic treatment with a wax-patterned, paper-based microfluidic device and demonstrate in-line quantification of the intraerythrocytic analyte hemoglobin without the use of a hemolytic buffer. We identified saponin as the optimal surfactant for in situ hemolysis because it does not denature proteins and is compatible with hydrophobic wax barriers. While saponin is commonly used in commercially available hemolytic buffers, this is the first demonstration of dried saponin stored within a paper-based device. Inclusion of a plasma separation membrane removes RBC membrane fragments to prevent clogging and treating the device with EDTA ensures proper transport of samples ranging from 20–55% hematocrit. Our paper punch and elution method allow for accurate determination of extent of hemolysis as a function of saponin stored in the device. The optimal treatment for maximum hemolysis is 10.6 μg saponin/cm^2 for samples ranging from 20–50% hematocrit. Although we did not achieve quantitative hemolysis for samples with higher hematocrit values we attribute this to inadequate rehydration of the dried saponin in the presence of increased

numbers of RBCs. However, incomplete hemolysis can be sufficient for a number of assay including diagnostic parasitic infections [38, 39]. Additionally, a correction factor could possibly be applied to quantitative results to account for lesser extent of hemolysis if the hematocrit value is known, which would be helpful with measuring hemoglobin A1c, glucose-6-phosphate-dehydrogenase activity, and total folate [40, 41]. Establishing a relationship between the amount of saponin and area allows this treatment to be translated to other devices with different geometries, potentially scaling device size down to use less blood [42].

5. Conflicts of Interest

The authors declare no conflicts of interest.

6. Acknowledgements

The project described was supported by the Tufts University Office of the Vice Provost for Research (OVPR) Research and Scholarship Strategic Plan (RSSP). This work was further supported by a generous gift from James Kanagy. The Advanced Light Source is supported by the Director, Office of Science, Office of Basic Energy Sciences, of the U.S. Department of Energy under Contract No. DE-AC02-05CH11231. We thank Dr. Syrena Fernandes, Christopher Luby, and Kirsten Deprey for their insight and assistance with experimentation.

7. Electronic supplementary information (ESI) available.

Figure 1. Schematic of a three-dimensional, paper-based device for in situ hemolysis and the quantification of hemoglobin. (A) Workflow for our elution method for quantification of hemoglobin in a paper-based device. (B) Schematic of a paper-based device for in situ hemolysis. Black areas are hydrophobic barriers prepared by wax printing. The dotted line represents the flow of sample through the device. Adhesive films between each layer are removed to simplify the illustration. We removed the terminal zone of the lateral channel (outlined in red) using a standard office punch (6-mm diameter) prior to the elution step. (C) Calibration curves for the quantification of hemoglobin. The calibration curves for both reference (red) and elution (blue) methods were constructed using hemoglobin standards (3–18 g/dL). Each data point is the mean of five replicates and the error bars represent the standard error of the mean. Each data set is fit using linear regression (reference method: R^2=0.997, slope=0.0127; elution method: R^2=0.995, slope=0.0101).

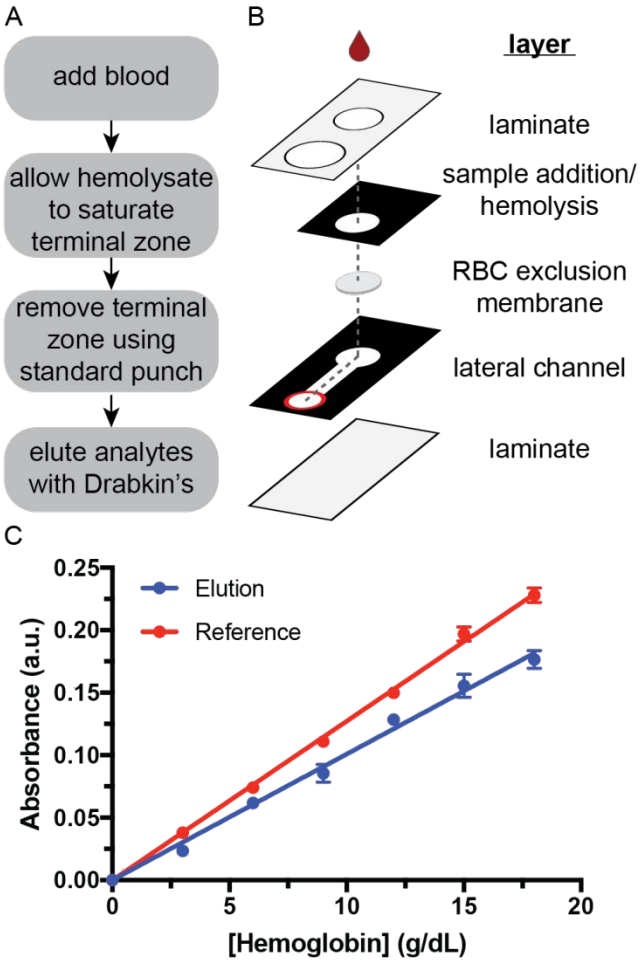
A
add blood
allow hemolysate to saturate terminal zone
remove terminal zone using standard punch
elute analytes with Drabkin's
B
layer
laminate
sample addition/ hemolysis
RBC exclusion membrane
lateral channel
laminate
C
Elution
Reference
Absorbance (a.u.)
0.25
0.20
0.15
0.10
0.05
0.00
0
5
10
15
20
[Hemoglobin] (g/dL)

Figure 2. Estimation of sample volume eluted from a 6-mm paper punch. The Drabkin's assay was performed using various sample volumes of hemoglobin standards (2, 3, 4, and 5 µL) in 1 mL of Drabkin's reagent. Calibration curves were generated over the physiological range of hemoglobin (3–18 g/dL) and the slope for each sample volume was plotted. The data are fit using linear regression (slope=0.0039, intercept=-0.0006, R^2=1.000) and error bars represent the estimated error of each slope at the 95% confidence interval.

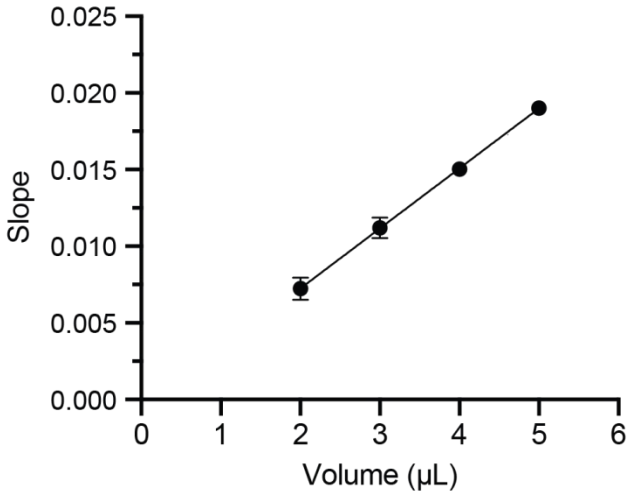

Figure 3. Determination of sample input volume using hemolysate controls. Samples of whole blood at various hematocrits (25–55%) were fully lysed and then applied to 0.5 M EDTA treated and untreated devices to simulate in situ quantitative hemolysis. In the absence of EDTA, hemolysate samples do not reach the end of the channel. In the presence of EDTA, hemolysate samples reach the end of the channel only when 40 µL of sample is applied across various hematocrits.

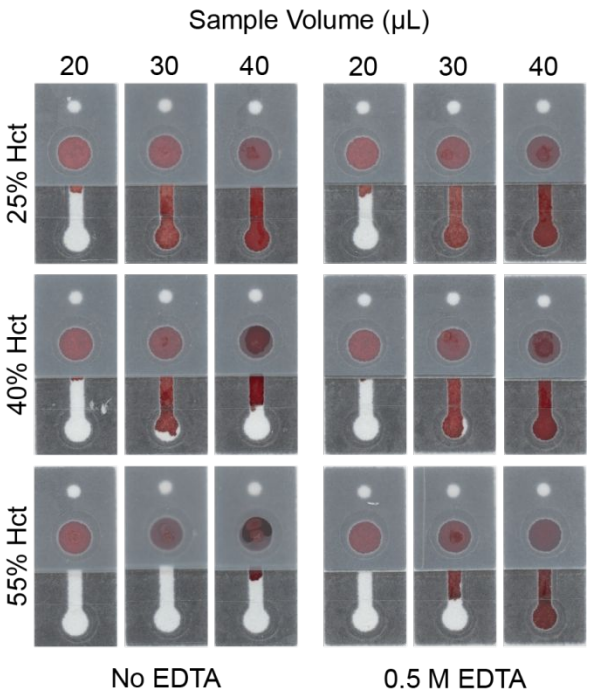

Figure 4. Evaluation of in situ hemolysis using blood at various hematocrits. (A) A sample of blood was prepared over a range of hematocrits (20–50%) and applied to paper-based devices treated with a varying concentration of saponin. Maximum extent of hemolysis was achieved for each sample in the presence of 10.6 µg saponin/cm^2. Each data point is the mean of five replicates and the error bars represent the standard error of the mean. (B) The total concentration of hemoglobin (g/dL), maximum extent of hemolysis (%), and standard error of the mean (%) is reported for each sample of blood under optimal hemolysis conditions.

A

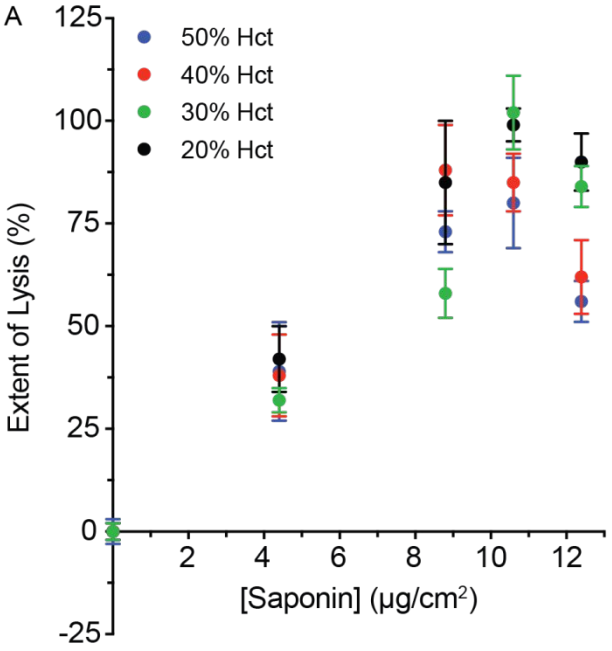

B

Hct	[Hgb] (g/dL)	Extent of Lysis	SEM
20%	6.5	99%	4%
30%	9.9	98%	9%
40%	14.8	85%	7%
50%	16.3	80%	11%

References

[1] Nayak S, Blumenfeld NR, Laksanasopin R, Sia SK. Point-of-care diagnostics: recent developments in a connected age. Anal Chem. 2017;89:102–123.

[2] Fernandes SC, Walz JA, Wilson DJ, Brooks JC, Mace CR. Beyond wicking: expanding the role of patterned paper as a foundation for an analytical platform. Anal Chem. 2017;89:5654–5664.

[3] Mahato K, Srivastava A, Chandra P. Paper based diagnostics for personalized health care: emerging technologies and commercial aspects. Biosens and Bioelectron. 2017;96:246–259.

[4] Sher M, Zhuang R, Demirci U, Asghar W. Paper-based analytical devices for clinical diagnosis: recent advances in the fabrication techniques and sensing mechanisms. Expert Rev Mol Diagn. 2017;17:351–366.

[5] Pandey CM, Augustine S, Kumar S, Kuma S, Nara S, Srivastava S, Malhotra BD. Microfluidics based point-of-care diagnostics. Biotechnol. 2018;13:1700047.

[6] Mariella R. Sample preparation: the weak link in microfluidics-based biodetection. Biomed Microdevices. 2008;10:777.

[7] Piety NZ, Yang X, Lezzar D, George A, Shevkoplyas SS. A rapid paper-based test for quantifying sickle hemoglobin in blood samples from patients with sickle cell disease. Am J Hematol. 2015;90:478–482.

[8] Horst AL, Rosenbohm JM, Kolluri N, Hardick J, Gaydos CA, Cabodi M, Klapperich CM, Linnes JC. A paperfluidic platform to detect Neisseria gonorrhoeae in clinical samples. Biomed Microdevices. 2018;20:35.

[9] Deraney RN, Mace CR, Rolland JP, Schonhorn JE. Multiplexed, patterned-paper immunoassay for detection of malaria and dengue fever. Anal Chem. 2016;88:6161–6165.

[10] Cheung SF, Yee MF, Le NK, Wu BM, Kamei DT. A one-pot, isothermal DNA sample preparation and amplification platform utilizing aqueous two-phase systems. Anal Bioanal Chem. 2018;410:5255–5263.

[11] Di Carlo D, Jeong KH, Lee LP. Reagentless mechanical cell lysis by nanoscale barbs in microchannels for sample preparation. Lab Chip. 2003;3:287–291.

[12] Pham VTH, Truong VK, Mainwaring DE, Guo Y, Baulin VA, Al Kobaisi M, Gervinskas G, Juodkazis S, Zeng WR, Doran PP. Nanotopography as a trigger for the microscale, autogenous and passive lysis of erythrocytes. J Mater Chem B. 2014;2:2819–2826.

[13] Baek S, Min J, Park JH. Wireless induction heating in a microfluidic device for cell lysis. Lab Chip. 2010;10:909–917.

[14] Buser JR, Diesburg S, Singleton J, Guelig D, Bishop JD, Zentner C, Burton R, LaBarre P, Yager P, Weigl BH. Precison chemical heating for diagnostic devices. Lab Chip. 2015;15:4423.

[15] Buser JR, Zhang X, Byrnes SA, Ladd PD, Heiniger EK, Wheeler MD, Bishop JD, Englund JA, Lutz B, Weigl, BH. A disposable chemical heater and dry enzyme preparation for lysis and extraction of DNA and RNA from microorganisms. Anal Methods. 2016;8:2880–2886.

[16] Kashyap A, Autebert J, Delamarche E, Kaigala GV. Selective local lysis and sampling of live cells for nucleic acid analysis using a microfluidic probe. Sci Rep. 2016;6:29579.

[17] Jen CP, Hsiao JH, Maslov NA. Single-cell chemical lysis on microfluidic chips with arrays of microwells. Sensors. 2012;12:347–358.

[18] Beyor N, Seo TS, Liu P, Mathies RA. Immunomagnetic bead-based cell concentration microdevice for dilute pathogen detection. Biomed Microdevices. 2008;10:909.

[19] Islam MS, Aryasomayajula A, Selvaganapathy PR. A review on macroscale and microscale cell lysis methods. Micromachines. 2017;8:83.

[20] Schonhorn JE, Fernandes SC, Rajaratnam A, Deraney RN, Rolland JP, Mace CR. A device architecture for three-dimensional, patterned paper immunoassays. Lab Chip. 20014;14:4653–4658.

[21] Altundemir S, Uguz AK, Ulgen K. A review on wax printed microfluidic paper-based devices for international health. Biomicrofluidics. 2017;11:041501.

[22] Channon RB, Nguyen MP, Henry CS, Dandy DS. Multilayered microfluidic paper-based devices: characterization, modeling, and perspectives. Anal Chem. 2019;91:8966–8972.

[23] Fernandes SC, Logounov GS, Munro JB, Mace CR. Comparison of three indirect immunoassay formats on a common paper-based microfluidic device architecture. Anal Meth. 2016;8:5204–5211.

[24] Fernandes SC, Walz JA, Wilson DJ, Brooks JC, Mace CR. Beyond wicking: expanding the role of patterned paper as a foundation for an analytical platform. Anal Chem. 2017;89:5654–5664.

[25] Tang R. Yang H, Ru Choi J, Gong Y, Hu J, Wen T, Li X, Xu B, Mei Q, Xu F. Paper-based device with on-chip reagent storage for rapid extraction of DNA from biological samples. Microchim Acta. 2017;184:2141–2150.

[26] Govindarajan AV, Ramachandran S, Vigil GD, Yager P, Bohringer KF. A low cost point-of-care viscous sample preparation device for molecular diagnosis in the developing world; an example of microfluidic origami. Lab Chip. 2012;12:174.

[27] BinaxNOW Malaria Test Kit Laboratory Procedure. Abbott. 2017. Accessed 29 Aug 2019.

[28] Baumann E, Stoya G, Volkner A, Richter W, Lemke C, Linss W. Hemolysis of human erythrocytes with saponin affects the membrane structure. Acta Histochem. 2000;120:21–35.

[29] Helenius A, Simons K. Solublization of membranes by detergents. Biochim Biophys Acta. 1975;415:29–79.

[30] Murray LP, Baillargeon KR, Bricknell JR, Mace CR. Determination of sample stability for whole blood parameters using formal experimental design. Anal Methods. 2019;11:930–935.

[31] WHO manual for HIV drug resistance testing using dried blood spot specimens. World Health Organization. 2010. Accessed 11 Aug 2019.

[32] Drabkin's reagent product information. Sigma-Aldrich. 2015. Accessed 29 Aug 2019.

[33] Carrilho E, Martinez AW, Whitesides GM. Understanding wax printing: a simple micropatterning process for paper-based microfluidics. Anal Chem. 2009;81:7091–7095.

[34] Berry SB, Fernandes SC, Rajaratnam A, DeChiara NS, Mace CR. Measurement of the hematocrit using paper-based microfluidic devices. Lab Chip. 2016;16:3689–3694.

[35] Zenyuk IC, Lamibrac A, Eller J, Dilworth PY, Marone F, Buchi FN, Weber AZ. Investigating evaporation in gas diffusion layers for fuel cells with X-ray computed tomography. J Phys Chem C. 2016;120:28701–28711.

[36] Zenyuk IV, Parkinson DY, Connolly LG, Weber AZ. Gas-diffusion-layer structural properties under compression vai X-ray tomography. J Power Sources. 2016;328: 364–376.

[37] Precision woven synthetic monofilament fabrics. SEFAR PETEX. 2015. Accessed 20 Nov 2019.

[38] Reboud J, Xu G, Garrett A, Adriko M, Yang Z, Tukahebwa EM, Rowell C, Cooper JM. Paper-based microfluidics for DNA diagnostics of malaria in low resource underserved rural communities. PNAS. 2019;116:4834–4842.

[39] Mosqueda J, Olvera-Ramirez A, Aguilar-Tipacamu G, Canto GJ. Current advances in detection and treatment of babesiosis. Curr Med Chem. 2012;19:1504–1518.

[40] Lippi G, Plebani M. Recent developments and innovations in red blood cells diagnostics. J Lab Precis Med. 2018;3:68.

[41] Pirkle JL. Total folate laboratory procedure manual. Centers for Disease Control. 2012. Accessed 30 Sept 2019.

[42] Fernandes SC, Baillargeon KR, Mace CR. Reduction of blood volume required to perform paper-based hematocrit assays guided by device design. Anal Methods. 2019;11:2057–2063.

Table of Contents Figure. Quantitative in situ hemolysis is achieved for samples of whole blood using a chemical treatment without additional user-steps or sample preparation.